2015 IEEE 28th International Symposium on Computer-Based Medical Systems

Use of Wavelet Multiresolution Analysis to Reduce Radiation Dose in Digital Mammography

Helder C. R. de Oliveira*, Lucas R. Borges*, Polyana F. Nunes*, Predrag R. Bakic**, Andrew D. A. Maidment**, Marcelo A. C. Vieira*
* Department of Electrical Engineering, University of São Paulo, São Carlos, Brazil
** Department of Radiology, University of Pennsylvania, Philadelphia, USA
{heldercro, lucas.rodrigues.borges, polyananunes}@usp.br
{predrag.bakic, andrew.maidment}@uphs.upenn.edu
{mvieira}@sc.usp.br

***Abstract*—This paper investigates the use of a wavelet multiresolution analysis to reduce noise in mammographic images acquired with low levels of radiation dose. We studied the use of a wavelet denoising technique to filter the quantum noise that is incorporated in mammographic images when the radiation dose is reduced. Results were obtained by denoising a set of mammographic images acquired with different levels of radiation exposure, using an anthropomorphic breast phantom. Parameters of the algorithm were adjusted to provide more efficient reduction of noise without blurring or insertion of artifacts. We used the Anscombe transformation before denoising to convert the Poisson signal-correlated noise into an approximately additive white Gaussian noise. Evaluation of denoising performance were conducted by comparing image quality indexes between mammograms acquired with normal radiation dose and those acquired at lower doses levels, after denoising by the proposed technique.**

Keywords-component; image processing; image denoising; digital mammography; quantum noise; wavelet transform; Anscombe transformation.

I. Introduction

Digital mammography is the most important exam to early detection of breast cancer, with a better performance than the screen-film mammography [1]. However, nowadays the radiation doses used in clinical practice with the digital systems are approximately the same used by the screen-film systems. It happens because the relationship between the radiation dose and the accuracy of medical diagnosis is not yet well established for digital mammography [2].

It is known the radiation exposure caused by mammography exams can induce the development of breast cancer in some women undergoing mammographic screening [3,4]. The main obstacle to reducing the radiation dose in mammography is the increase of quantum noise in the image. The quantum noise is the result of low photon count used in image formation process; it is the main cause of the reduction of visibility of subtle lesions in mammography [5]. Thus, a reduction in the radiation dose and the consequent increase in image noise may compromise the detection of breast lesions by radiologists, especially in its early stages [2].

Accordingly, the aim of this study is to investigate the use of denoising techniques to reduce the quantum noise in mammographic images acquired with reduced radiation dose, providing that the image quality is preserved as for the images acquired at the standard dose. The denoising technique proposed in this work is the coefficient shrinkage in wavelet domain, a method that uses the multiresolution concept to remove noise of digital images [6]. The denoising process was applied to a set of mammographic images acquired in different radiation levels in a clinical mammographic unit, using an anthropomorphic breast phantom [7,8]. As the wavelet shrinkage methodology has been proposed by Additive White Gaussian Noise (AGWN), we used the Anscombe Transformation [9,10,11] in order to stabilize the variance of signal prior to denoising, converting the signal-dependent Poisson noise into an approximately AGWN.

II. Materials and Methods

A. Noise Filtering

The observation of an image $g(x)$ corrupted by AGWN, where x is the 2D spatial coordinate of image pixels, is defined by:

$$g(x) = f(x) + n(x), \quad (1)$$

where $f(x)$ is the noiseless image and $n(x)$ is the additive noise.

Denoising algorithms normally have the goal of calculating an estimate $\hat{f}(x)$ of the noiseless image $f(x)$ by removing noise from image $g(x)$ with minimum blurring or artifacts insertion.

In this work, the denoising algorithm used to allow a dose reduction in digital mammography follows the framework established by Donoho and Johnstone [12,13], which consists of three steps:

1. Decompose the input signal (I) with forward wavelet transform:

$$Y = W(I) \quad (2)$$

2372-9198/15 $3.00 © 2015 IEEE
DOI 10.1109/CBMS.2015.35

2. Apply a thresholding (D) method to the coefficients:

$$Z = D(Y, \lambda) \tag{3}$$

3. Apply the wavelet inverse transform in order to reconstruct the signal:

$$\hat{I} = W^{-1}(Z) \tag{4}$$

The wavelet transform consists in systematically applying the orthonormal bases pair, ϕ and ψ to the input signal. In the case of bi-dimensional signals, as images, the forward transform is applied alternately to the lines and columns of the signal. Thereby, the sub-bands produced are defined as:

$$\psi^H(x,y) = \psi(x) \times \phi(y) \tag{5}$$

$$\psi^V(x,y) = \phi(x) \times \psi(y) \tag{6}$$

$$\psi^D(x,y) = \psi(x) \times \psi(y) \tag{7}$$

$$\phi(x,y) = \phi(x) \times \phi(y) \tag{8}$$

where ψ^H, ψ^V, ψ^D and ϕ are the detail horizontal, detail vertical, detail diagonal and approximation coefficients, respectively.

In this work, we used the pair of bases developed by Ingrid Daubechies [14], with 4 vanishing moments, known by Db-4. These bases were chosen empirically.

The multilevel decomposition occurs when we apply the same approach to the approximation coefficients, which again can be decomposed on four more sub-bands. The coefficients generated by wavelet decomposition permit better separability between the original signal (which is represented by coefficients of greater magnitude and smaller quantities) and the noise (which are represented by coefficients of smaller magnitude and greater quantity).

We can explore the separability of the signals in wavelet domain to better noise filtering: a thresholding procedure should be applied to the details coefficients (horizontal, vertical and diagonal) to remove noise coefficients and preserve the original signal of the image. In the literature, the most used procedures are the hard and soft thresholding [14,15]. However, given the approach of this work, the best performance was obtained with a customized threshold rule we designed specifically to remove noise in digital mammography:

$$D_L(Y,\lambda,F) = \begin{cases} Y, & \text{if } |Y| > \lambda \\ Y \times F, & \text{otherwise} \end{cases} \tag{9}$$

where Y corresponds to the input signal, λ is the threshold value and, F is a scale factor.

The main idea was to remove the spare noise that was added to the images when acquired with low doses of radiation. Thus, the scale factor added conducts a gradual reduction of the coefficient according to its magnitude, which is related to image noise (and consequently the radiation dose). Whether the coefficients have a relatively small magnitude, this rate will converge to zero naturally.

Besides the threshold rule to be used, the success of filtering is dependent on a good estimate of the threshold value λ. In this sense, the literature contains a wide range of techniques [12,13,15]. In this work, we used the *VisuShrink*, technique [12], described in (10). It was chosen for its simplicity and for being a good estimator:

$$\lambda = \sqrt{2 \times logN} \times \sigma \tag{10}$$

where, N is the total amount of elements to be processed and σ is the noise standard deviation.

Images were decomposed in five levels for the proposal of this work. As each level of decomposition produces three details sub-bands, the threshold rule as well as the estimate of λ was applied locally in each one of them.

Regarding the noise characteristics in digital mammography, it is known that the predominant noise in mammographic images is the quantum noise [2,5], which is non-additive, signal-dependent and can be described by Poisson's probability mass function:

$$p(k) = \frac{e^{-\lambda}\lambda^k}{k!}, \tag{11}$$

where k is a random variable and λ is the expected value of the Poisson distribution, which is in this case equal to the mean and the variance of the distribution.

Thus, in order to work with additive and non-correlated noise from a Poisson noise, we must use a *Variance Stabilization Transformation* (VST) to convert Poisson noise into AWGN. In this work we used the *Anscombe Transformation* [9,10,11], given by (12), which is one of the most known VST and can convert an image $g(x)$ corrupted by Poisson noise in an image corrupted by approximately AWGN, with zero mean and unit variance:

$$\mathrm{z}(x) = 2\sqrt{g(x) + \frac{3}{8}}, \tag{12}$$

It has been proved that the inverse algebraic Anscombe transformation is biased. For this work, we used the inverse transformation proposed by [16], which shows to be exact and asymptotically unbiased.

B. *Mammographic Images*

The tests were performed through a set of mammographic images acquired in a clinical mammographic machine (Selenia Dimensions, Hologic, Bedford, MA) under four different levels of radiation exposures, in order to simulate different quantities of quantum noise. We acquired 20 mammographic images in dose levels corresponding to 100%, 85%, 70% and 50% of a standard radiation dose used clinically (5 images in each dose level). All image acquisitions were performed using an anthropomorphic physical breast phantom [7] prototyped by CIRS, Inc. (Reston, VA) based upon a realization of the breast software phantom developed at the University of Pennsylvania [8]. The use of a physical phantom was important to assure that all images acquisitions had the same object in the same position. Fig. 1 shows a picture of the physical phantom used in this work (in the left) and the corresponding mammographic image of the phantom (in the right).

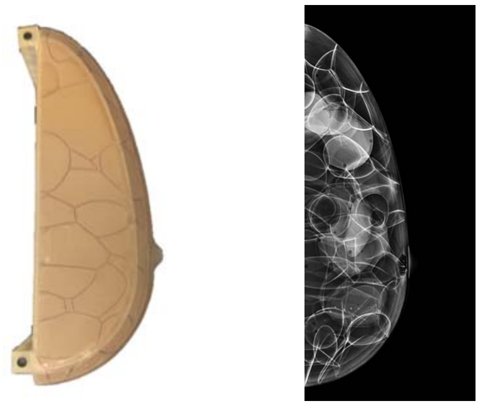

(a) (b)

Figure 1. (a) in the left: Anthropomorphic breast phantom used in this study; (b) in the right: example of a mammographic image acquired in a clinical machine using this phantom.

Fig. 2 shows ROIs extracted from the images acquired in different dose levels: 100%, 85%, 70% and 50% of the standard dose, respectively. As the images came from the same phantom, they have exactly the same tissue structures and microcalcifications, but different levels of quantum noise.

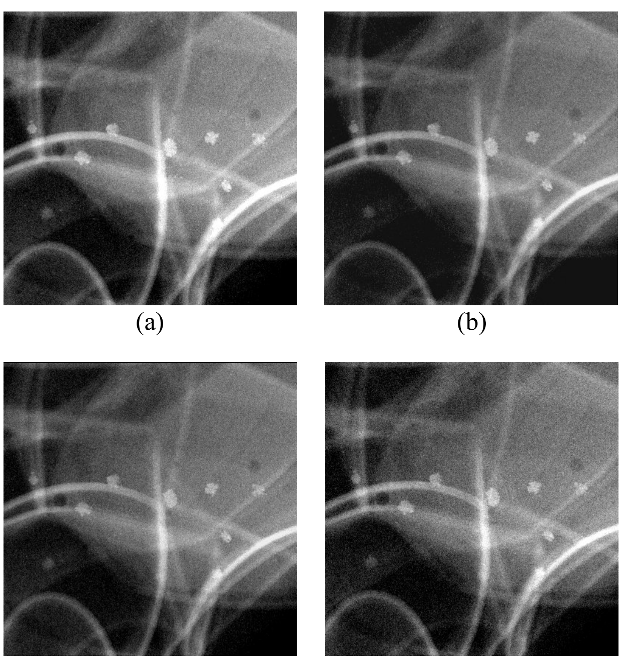

(a) (b)

(c) (d)

Figure 2. Region of interest showing a cluster of microcalcifications extracted from the mammographic images acquired at different dose levels: (a) 100%, (b) 85%, (c) 70%, and (d) 50% of the regular dose.

In addition to these images, we created an additional set of 10 images that were acquired using regular dose levels (100%). These images were averaged to have the noise removed, creating a reference image (ground-truth). Since noise is a random event, averaging several images can provide a good estimate of a noiseless image. Ground-truth images are important for the image quality assessment.

C. *Evaluation of Denoising Methodology*

The evaluation of the proposed technique was performed using quantitative image quality metrics. We measured the Peak Signal-to-Noise Ratio (PSNR) [17] and the Mean Structural Similarity Index (MSSIM) [18] for all images used in this study, before and after the use of the denoising technique.

III. Results and Discussion

The assessment of the proposed methodology were conducted considering the following approach:

1. The same ROI of $400 \, x \, 400$ pixels was extracted from all mammographic images, considering the same spatial coordinates. Each ROI was evaluated in terms of PSNR and MSSIM, before applying the denoising methodology.
2. For each ROI of 50%, 70% and 85% of dose, we applied the proposed denoising methodology. Filter parameters were adjusted considering that the low-dose images must have same quality than the 100% image.
3. After denoising, we calculated the same image quality measurements again.
4. The results before and after the denoising were comparing in order to evaluate the performance of the proposed noise attenuation methodology.

Using the ROIs of each realization in each dose, the evaluation using images quality metrics (PSNR and MSSIM) was performed and at the end the values of all results were averaged. The results of each dose are presented in Table 1.

Table 1. Average values of image quality indexes calculated for the all images in each dose and its respective standard deviation.

Relative Dose	PSNR (dB)	MSSIM
100%	39.01 ± 0.07	0.8975 ± 0.0013
85%	38.57 ± 0.05	0.8877 ± 0.0010
70%	37.96 ± 0.05	0.8728 ± 0.0012
50%	36.28 ± 0.06	0.8233 ± 0.0017

Fig. 3 shows graphically the results presented in Table 1. It is possible to see how the reduction of the radiation dose can degrade image quality in terms of PSNR and MSSIM values.

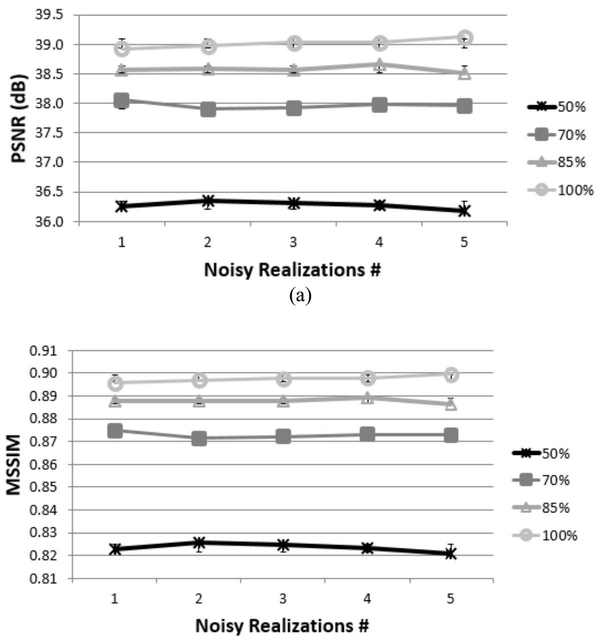

(a)

(b)

Figure 3. Values of five realizations of each dose in terms of (a) PSNR (dB) and (b) MSSIM before denoising

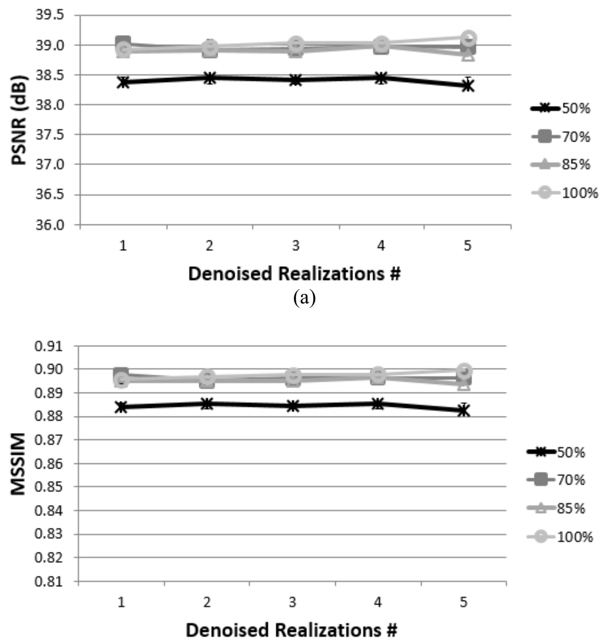

(a)

(b)

Figure 4. Values of five realizations of each dose, after applying the denoising method, in terms of (a) PSNR (dB) and (b) MSSIM.

Considering this preliminary evaluation it was possible to establish a goal, that is, how to filter the low-dose images in order to have the same quality than the images acquired with regular radiation dose (100%).

The proposed denoising method can be adjusted to find the best value for the scale factor F (9) used in the shrinkage of the detail coefficients. Empirically, those values were found and are presented in Table 2, where the shadowed line contains the target values.

Table 2. Evaluation, after filtering, of average the assessments metrics of five realizations in each dose, its respective standard deviation and factor value used.

Dose	PSNR (dB)	MSSIM	Factor (F)
100%	39.01 ± 0.07	0.8975 ± 0.0013	-
85%	38.90 ± 0.05	0.8950 ± 0.0011	0.95
70%	38.95± 0.04	0.8963 ± 0.0008	0.85
50%	38.40± 0.06	0.8843 ± 0.0011	0.70

Fig. 4 shows graphically the results presented in Table 2. It is possible to see how the proposed denoising methodology removed noise from the low-dose images in order to present same quality indexes. We can notice that after denoising all images acquired in lower dose levels became more similar, considering PSNR and MSSIM measurements.

The same ROIs showed at Fig. 2, before denoising, are now presented, at Fig. 5, after denoising. Is possible to see that all ROIs have the same noise level and all microcalcifications were preserved in the image.

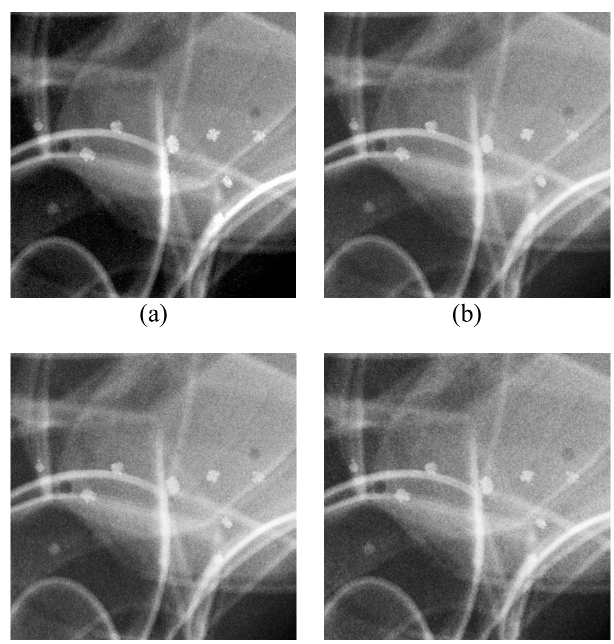
(a) (b)

(c) (d)

Figure 5. Region of interest showing a cluster of microcalcifications extracted from the mammographic images acquired at different dose levels, after denoising by the proposed methodology: (a) 100%, (b) 85%, (c) 70%, and (d) 50% of the regular dose.

IV. CONCLUSIONS

Normally, denoising algorithms in wavelet domain aim to remove most of the noise of digital images. However, in this work, we investigated the use of wavelet transform as a tool to allow a reduction of the radiation dose in digital mammography. A pre-clinical study using anthropomorphic phantom images were conducted and we obtained promising results. Results showed that it is possible to remove the quantum noise added to the image when the radiation dose is reduced to 85%, 75%, and 50% of the standard dose provided for our physical phantom. The assessment of denoised images using image quality metrics such as PSNR and MSSIM confirms that the image quality in images acquired with lower radiation dose may preserve image quality.

Since quantum noise is signal-dependent, the Anscombe transformation came to be a vital tool to perform a better filtering without blurring the image and therefore compromise the diagnosis. Related works on the denoising of mammographic images using the Anscombe transformation can be found in [10,11].

Despite of the results obtained in this work, it is necessary to go further to better evaluate clinical images in terms of blur and how they can affect medical diagnosis, as well as establish a methodology where the *F* parameter will be defined automatically according to the radiation dose used in image acquisition.

ACKNOWLEDGMENT

This work was supported by the São Paulo Research Foundation (FAPESP) grant #2013/18915-5, by the Brazilian Foundation for the Coordination of Improvement of Higher Education Personnel (CAPES) and by the US National Institutes of Health (NIH): R01 grant #CA154`444. The content is solely the responsibility of the authors and does not necessarily represent the official views of the NIH, CAPES or FAPESP.

REFERENCES

[1] Glynn CG, Farria DM, Monsees BS, Salcman JT, Wiele KN Hildebolt CF: "Effect of transition to digital mammography on clinical outcomes". Radiology 260(3):664-670, 2011.

[2] Samei E, Saunders RS, Baker JA, Delong DM: "Digital mammography: effects of reduced radiation dose on diagnostic performance", Radiology 243(2):396-404, 2007.

[3] Hendrick RE: "Radiation doses and cancer risks from breast imaging studies", Radiology 257(1):246-253, 2010.

[4] Yaffe MJ, Mainprize, JG: "Risk of radiation-induced breast cancer from mammographic screening", Radiology 258(1):98-105, 2011.

[5] Yaffe MJ: "Digital Mammography". In: Beutel J, Kundel HL and Van Metter RL (Eds). Handbook of Medical Imaging Vol 1. Physics and Psychophysics, Bellingham, WA: SPIE Press, pp 329-372, 2000.

[6] Taswell C: "The what, how, and why of wavelet shrinkage denoising". Computing in Science & Engineering 2(3):12-19, 2002.

[7] Cockmartin L, Bakic PR, Bosmans, H, Maidment, ADA, Gall H, Zerhouni M, and Marshall NW. "Power spectrum analysis of an anthropomorphic breast phantom compared to patient data in 2D digital mammography and breast tomosynthesis". In Fujita H, Hara T, Muramatsu C (eds), Breast imaging (IWDM), LCNS 8539: Berlin Heidelberg: Springer-Verlag; 2014.

[8] Pokrajac DD, Maidment ADA, Bakic PR. Optimized generation of high resolution breast anthropomorphic software phantoms. Med Phys 39(4):2290–2302; 2012.

[9] Anscombe FJ: "The transformation of Poisson, binomial and negative-binomial data". Biometrika vol. 35, pp. 246–254, 1948.

[10] Vieira MAC, Bakic PR, Maidment ADA, Schiabel H, Mascarenhas NDA. "Filtering of poisson noise in digital mammography using local statistics and adaptive Wiener Filter". Proc. of 11th International Workshop on Breast Imaging, LNCS7361, 268-275, 2012.

[11] Vieira MAC, Bakic PR, Maidment ADA, "Effect of denoising on the quality of reconstructed images in digital breast tomosynthesis", Proc. of SPIE Vol. 8668(86680C), 2013.

[12] Donoho DL, Johnstone IM: "Adapting to unknown smoothness via wavelet shrinkage". Technical report, Department of Statistics, Stanford University, 1992.

[13] Donoho DL, Johnstone IM: "Ideal spatial adaptation via wavelet shrinkage". Technical report, Stanford University, 1992.

[14] Daubechies I: "Ten lectures on wavelets". Society for Industrial and Applied Mathematics, 1992.

[15] Mallat S: "A wavelet tour of signal processing, 3rd ed. Academic Press, 2008.

[16] Mäkitalo M, Foi A: "A closed-form approximation of the exact unbiased inverse of the Anscombe variance-stabilizing transformation". IEEE Tans. Image Process. 20(9): 2697-2698, 2011.

[17] Wang Z, Bovik AC: "Mean squared error: Love it or leave it? A new look at signal fidelity measures". IEEE Signal Proc. Mag. 26(1):98-117, 2009.

[18] Wang Z, Bovik AC, Sheikh HR, Simoncelli, EP: "Image quality assessment: from error visibility to structural similarity". IEEE Trans. Image Process. 13(4):600-612, 2004.